Physics Letters B 782 (2018) 768–772

Contents lists available at ScienceDirect

Physics Letters B

www.elsevier.com/locate/physletb

Observation of multiple doubly degenerate bands in ^{195}Tl

T. Roy [a,b], G. Mukherjee [a,b,*], Md.A. Asgar [a,b], S. Bhattacharyya [a,b], Soumik Bhattacharya [a,b], C. Bhattacharya [a,b], S. Bhattacharya [a,1], T.K. Ghosh [a,b], K. Banerjee [a,b,c], Samir Kundu [a,b], T.K. Rana [a], P. Roy [a,b], R. Pandey [a,b], J. Meena [a], A. Dhal [a], R. Palit [d], S. Saha [d], J. Sethi [d], Shital Thakur [d], B.S. Naidu [d], S.V. Jadav [d], R. Dhonti [d], H. Pai [e], A. Goswami [e]

[a] Variable Energy Cyclotron Centre, 1/AF, Bidhan Nagar, Kolkata - 700064, India
[b] Homi Bhaba National Institute, Training School Complex, Anushakti Nagar, Mumnai - 400094, India
[c] Department of Nuclear Physics, Research School of Physics and Engineering, Australian National University, Canberra, ACT 2601, Australia
[d] Tata Institute of Fundamental Research Centre, Colaba, Mumbai - 400005, India
[e] Saha Institute of Nuclear Physics, Kolkata 700064, India

ARTICLE INFO

Article history:
Received 12 May 2018
Received in revised form 10 June 2018
Accepted 14 June 2018
Available online 18 June 2018
Editor: V. Metag

Keywords:
Nuclear Structure
γ-ray spectroscopy
Doubly degenerate bands
TRS calculation

ABSTRACT

The High-spin states in ^{195}Tl, populated through the ^{185,187}Re(^{13}C, xn) fusion evaporation reaction at the beam energy of 75 MeV, were studied using the Indian National Gamma Array (INGA). More than 50 new γ transitions have been placed in the proposed level scheme which is extended up to the excitation energy of $\approx$ 5.6 MeV and spin = 22.5$\hbar$. Two pairs of degenerate bands based on two different quasi-particle configurations have been identified in this nucleus indicating the first observation of such bands in an odd-A nucleus in $A \sim 190$ region and signify the first evidence of multiple chiral bands in a nucleus in this region. The total Routhian surface calculations predict triaxial shapes for both the configurations and thereby, support the experimental observation. The importance of multiple neutron holes in the $i_{13/2}$ orbital and the stability of shapes for these two configurations have been discussed.

The atomic nuclei are considered as the fascinating quantal objects to study various symmetries in nature. Breaking of a particular symmetry in the nuclear medium is manifested in terms of different band structures of nuclear excited states. A new type of symmetry breaking for the triaxial nuclei with the unpaired particle(s) and hole(s) in the high-j orbital, referred as chiral symmetry breaking, was proposed by Frauendorf et al. [1,2]. Such a chiral geometry is manifested in the occurrence of a pair of nearly degenerate $\Delta I = 1$ bands. One of the first experimental evidences of this was reported in the $N = 75$ isotones [3]. Subsequently, such chiral doublet bands have been observed in several nuclei mostly for 2- and 3-quasiparticle (qp) configurations [4–7]. Very recently, evidence of chirality has been observed in multi-qp configurations of even–even nucleus ^{136}Nd [8]. The observation of such band structures provides the clear indication of triaxial shape in a nucleus.

Chiral bands based on different configurations in a nucleus are possible provided the configurations satisfy the underlying conditions [2]. Evidence of chiral doublet bands based on different configurations was found in ^{105}Rh [9,10]. However, the possibility of the occurrence of multiple chiral doublet bands in ^{106}Rh was predicted from the relativistic mean field (RMF) calculations by J. Meng et al. [11] and they used the acronym MχD for such bands. However, until now the experimental observation of such bands has been reported only in a few nuclei, ^{133}Ce [12], ^{136}Nd [8] and ^{78}Br [13]. A different kind of MχD band, based on the same configuration, has been reported in ^{103}Rh [14].

For the nuclei in the $A = 190$ mass region high-j $h_{9/2}$ and $i_{13/2}$ orbitals are available near the proton and the neutron Fermi levels and the even–even Hg core nuclei are predicted to be triaxial in nature [15]. Therefore, it was suggested in Ref. [1] that the nuclei in this region are as promising as in the $A = 130$ region for the observation of chiral doublet bands. Several chiral doublet bands have been observed in the $A = 130$ region including the MχD bands in ^{133}Ce but, surprisingly it remained illusive in the $A = 190$ region. Only recently, chiral doublet bands are reported in ^{194}Tl and ^{198}Tl based on 4- and 2-quasiparticle configurations, respectively [16–18].

In this Letter, we are reporting the observation of two pairs of chiral doublet bands in the odd-even nucleus ^{195}Tl involving

* Corresponding author at: Variable Energy Cyclotron Centre, 1/AF, Bidhan Nagar, Kolkata - 700064, India.
E-mail address: gopal@vecc.gov.in (G. Mukherjee).
[1] Raja Ramanna Fellow.

https://doi.org/10.1016/j.physletb.2018.06.033

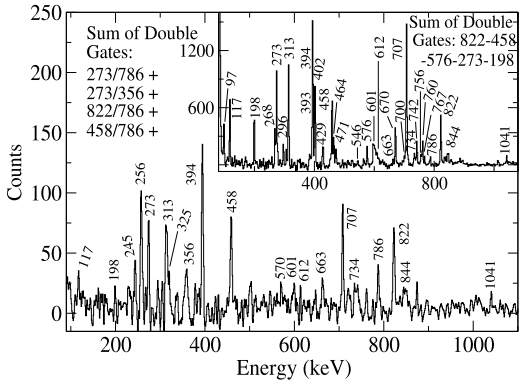

Fig. 1. Sum of double gated γ-ray coincidence spectra projected from the γ–γ–γ cube. The gates are chosen to show the γ-lines mainly in the newly observed bands B2 and B2a in ^{195}Tl. The inset shows the known and the new γ-lines in band B1.

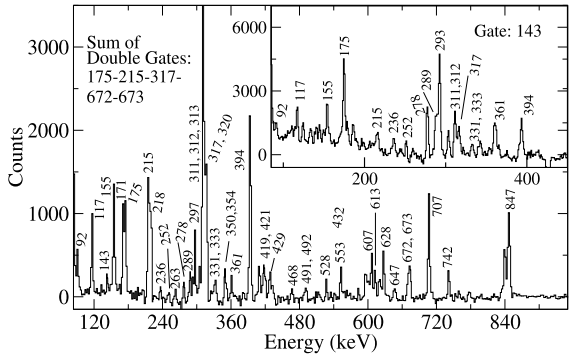

Fig. 2. Same as Fig. 1 but the gates are chosen to show the γ-lines mainly in the newly observed bands B4 and B4a in ^{195}Tl. A spectrum gated by one of the newly placed γ rays, 143 KeV, projected from the γ–γ matrix is shown in the inset. It shows the known γ lines in B3 and B4a and their connections to the low-lying states.

3-qp and 5-qp configurations representing the first evidence of true MχD bands based on different configurations in the same nucleus in the $A = 190$ region. Moreover, observation of chiral doublet bands based on configurations involving as large as 5-qp in this work is unique in a nucleus.

Prior to the present work, the high spin information for ^{195}Tl was limited to only two bands [19]: the 1-qp $\pi h_{9/2}$ band and a 3-qp band, known up to spin of $27/2^-$ and $35/2^+$ and excitation energy of 3156 and 4394 keV, respectively. These were measured using α induced fusion evaporation reaction with one planar Ge detector and two large volume Ge(Li) detectors. The present experimental condition is a much improved one as we have used heavy-ion induced fusion evaporation reaction and a much efficient germanium clover detector array to detect the γ-rays. These allowed us to populate higher spin states, to observe weakly populated states and to assign the spin and the parity of the states firmly.

The high spin states in ^{195}Tl were populated via the ^{185,187}Re(^{13}C, xn)^{195}Tl fusion evaporation reaction with a 75-MeV ^{13}C beam from the 14-UD Pelletron LINAC Facility at Tata Institute of Fundamental Research (TIFR), Mumbai, India. The prompt γ rays emitted from the residual nuclei were detected by the Indian National Gamma Array (**INGA**) facility with 15 Compton suppressed clover HPGe detectors. Two and higher-fold coincidence data with time stamp were recorded in a fast (100 MHz) digital data acquisition system based on the Pixie-16 modules of XIA LLC [20,21]. The experimental set up, the data acquisition conditions and the data analysis procedure have been described in Ref. [22].

A new and improved level scheme of ^{195}Tl with the placement of 57 new γ-rays, compared to the previous work [19], has been constructed by analyzing the intensity and coincidence relations of the γ-rays in the E_γ–E_γ matrix and the E_γ–E_γ–E_γ cube. A few of the gated spectra are shown in Fig. 1 and Fig. 2. A partial level scheme of ^{195}Tl, constructed by analyzing several such spectra, has been shown in Fig. 3. The previously known 1-qp and 3-qp bands B1 and B3 have been extended beyond the band crossing regions through the bands B2, B2a and B4, B4a, respectively.

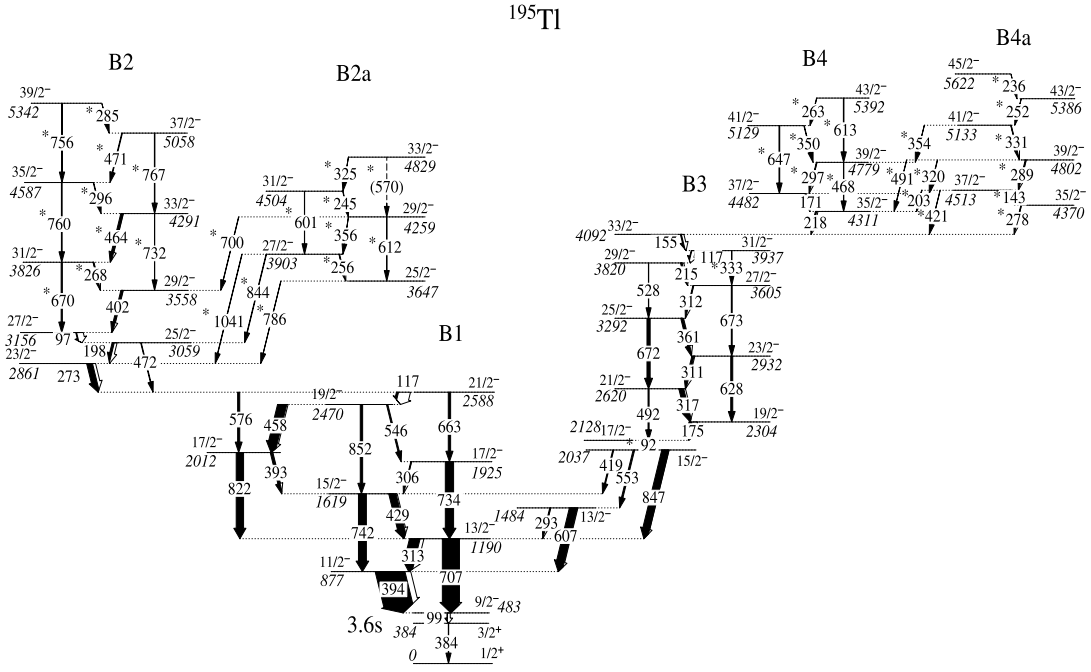

Fig. 3. Partial level scheme of ^{195}Tl proposed from the present work. The newly observed transitions are marked by asterisks (*). The width of the transitions are proportional to their intensity.

The spin and parity (J^{π}) of the states were unambiguously assigned in this work from the complete information on the multipolarity (λ) and the nature (E/M) of the γ rays decaying from a state by the integrated polarization asymmetry ratio (Δ_{IPDCO}) [23,24] and the directional correlation of oriented states ratio (R_{DCO}) [25] measurements as described in Ref. [22].

The configurations of the bands in the level scheme of ^{195}Tl are assigned by considering the measured gain in the aligned particle angular momentum (i_x), their comparison with the neighboring nuclei and, the available single particle orbitals near the proton and the neutron Fermi levels. The band B1 in ^{195}Tl and the similar bands in the neighboring odd-A Tl isotopes were known to be the rotational bands of an oblate deformed nucleus based on the odd proton in the $h_{9/2}$ orbital [19,26–29]. The newly observed 3-qp band B2 in ^{195}Tl is accompanied by a large gain of about 9$\hbar$ in i_x (see Fig. 4) indicating the alignment of a pair of neutrons in the high-j $i_{13/2}$ orbital. Therefore, this band has been assigned a configuration of $\pi h_{9/2} \otimes \nu i^{-2}_{13/2}$, the negative sign in the neutron configuration indicates the hole states. The value of i_x for the band B3 and B4 in ^{195}Tl closely match with the 5^- band in ^{194}Hg [30] both before and after the neutron pair alignments (Fig. 4). Hence, the neutron configuration of the band B3 and B4 would be similar to the 5^- band in ^{194}Hg. Considering the negative parity of the bands and the available orbitals near the proton Fermi level, the suggested configurations for the bands B3 and B4 in ^{195}Tl are $\pi i_{13/2} \otimes \nu i^{-1}_{13/2}(p_{3/2}f_{5/2})^{-1}$ and $\pi i_{13/2} \otimes \nu i^{-3}_{13/2}(p_{3/2}f_{5/2})^{-1}$, respectively.

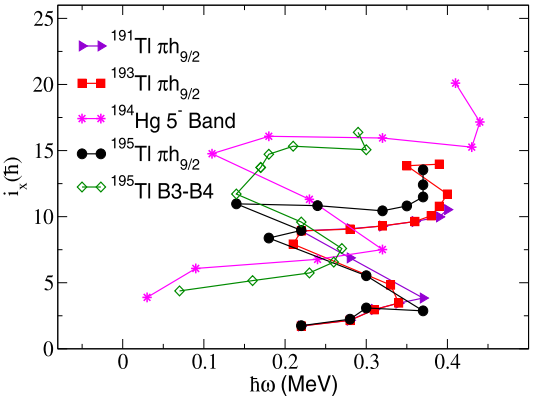

Fig. 4. Plot of the aligned angular momentum (i_x) as a function of rotatonal frequency ($\hbar\omega$) for the odd-A Tl and the even–even ^{194}Hg nuclei. The collective contributions, computed using the Harris reference parameters $J_0 = 8\hbar^2$ MeV^{-1} and $J_1 = 40\hbar^4$ MeV^{-3}, have been subtracted from each point.

In this letter, the primary focus is on the pair of bands B2 with its side band partner B2a and B4 with its side band partner B4a. These are identified as the closely degenerate pairs of bands as can be seen from their spin (I) vs. $E - E_{ref}$ (E is the excitation energy and $E_{ref} = A * I * (I + 1)$ is a rigid-rotor reference with A is the moment of inertia parameter) plots in Fig. 5(a). The i_x values (Fig. 5(b)) of the bands in a pair (B2 with B2a and B4 with B4a) are close to each other, indicating that the side bands have the same configuration as the main bands. Other parameters, like staggering (S(I)) and kinetic moment of inertia $J^{(1)}$, shown in Fig. 5(c) and (d), are also very similar. The B(M1)/B(E2) ratios for the bands B2-B2a and B4-B4a in ^{195}Tl match quite well too (Fig. 5(e)). These types of degenerate pair of bands, which have been interpreted as originated due to the chiral symmetry breaking in the angular momentum space in a triaxial nucleus [1,2], are comparable to those observed for the 4-qp configuration in ^{194}Tl [16,17] and the 2-qp configuration in ^{198}Tl [18]. The relevant parameters for these bands in ^{194,198}Tl are also compared in Fig. 5. It is seen that the degeneracies in ^{195}Tl are either similar or better compared to ^{194,198}Tl. The average separation of $\Delta E_{av} \sim 25$ keV (with the maximum value $\Delta E_{max} = 59$ keV) in the excitation energies for the 5-qp bands B4-B4a in ^{195}Tl is much less than $\Delta E_{av} \sim 78$ keV (with $\Delta E_{max} = 110$ keV) for the 4-qp bands in ^{194}Tl. Therefore, it represents one of the best examples of degenerate bands observed so far. The degeneracy in the 3-qp pair B2-B2a, is comparable with that reported for the 2-qp pair in ^{198}Tl.

The two pairs of doubly degenerate bands identified in ^{195}Tl is a unique observation in the $A = 190$ mass region. This is the first time that multiple pairs of candidate chiral partner bands are observed in this region and also identified for the first time for a configuration involving as large as 5 quasiparticles in a nucleus in

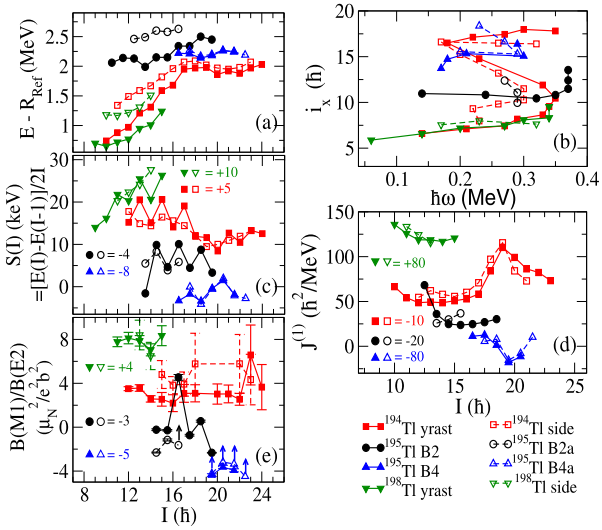

Fig. 5. (Color online.) Comparative study of various experimental parameters belonging to bands B2-B2a and B4-B4a in ^{195}Tl with those in the degenerate bands based on 2-qp and 4-qp configuration in ^{194,198}Tl isotopes. (a) Plot of excitation energy (E) with a rigid rotor reference ($E_{ref} = A * I * (I + 1)$, where A is the moment of inertia parameter and I is the spin) subtracted vs. spin (I). (b) Plot of single particle alignment (i_x) vs. rotational frequency ($\hbar\omega$). The Harris reference parameters were taken as $J_0 = 8\hbar^2$ MeV^{-1} and $J_1 = 40\hbar^4$ MeV^{-3}. (c) Plot of energy staggering $S(I) = [E(I) - E(I-1)]/2I$ vs. spin(I). (d) Plot of kinematic moment of inertia ($J^{(1)}$) vs. spin(I) and (e) Plot of the ratio of transition probabilities B(M1)/B(E2) vs. spin(I). For visual convenience some of the plots are shifted in y-axis. The amount of shifts given to different plots are mentioned inside each graph.

this mass region. This is a valuable addition to the ones reported for ^{133}Ce and in ^{78}Br [12,13] in a different mass region which gives a strong support and general applicability to the recent theoretical prediction of multiple chiral doublet (MχD) bands and triaxial shapes involving different configurations in a nucleus [2,11].

The chiral geometry, in this case, is generated with the angular momentum of the valence proton (neutron) particle (hole) aligned along the short (long) nuclear axes and core rotational angular momentum predominantly oriented along the intermediate nuclear axis. For this to happen, the nucleus must be triaxial in shape. A chiral geometry is better realized in a nucleus having stable triaxial shape with triaxiality parameter γ lies between $25^\circ < |\gamma| < 40^\circ$ [1]. Degenerate chiral doublet bands are most favorable for maximum triaxiality ($|\gamma| = 30^\circ$). It was also reported that for a γ-soft nucleus, the aplanar solution (which gives chiral side band) disappears and destroys the chirality [31]. In case of ^{195}Tl, it turns out that the 5-qp configuration seems to have a rather stable triaxial shape than the 3-qp one. This indicates that as the number of unpaired neutron holes increases in the $i_{13/2}$ orbital, it drives the nucleus to a more stable triaxial deformation.

In order to estimate the shape of ^{195}Tl nucleus in the above mentioned configurations, the total Routhian surface (TRS) calculations have been performed. The TRS code of Nazarewicz et al. [32,33] was used in these calculations. The procedure of such calculations has been outlined in Ref. [34,35]. The Routhian surfaces are plotted in the conventional $\beta_2 - \gamma$ plane and are shown in Fig. 6. In these plots, $\gamma = 0^0$ ($\gamma = -60^0$) corresponds to prolate (oblate) shape. Triaxial shapes correspond to γ in between these two values with $\gamma = \pm 30^\circ$ represents maximum triaxiality.

The surface calculated for the $\pi h_{9/2}$ configuration corresponding to the band B1 (Fig. 6(a)) in ^{195}Tl shows an axially symmetric oblate deformation with $\beta_2 = 0.15$ and $\gamma = -58^0$. Whereas, triaxial minimum appears for the 3-qp and the 5-qp configurations corresponding to bands B2 and B4, respectively, with $\gamma \sim +30^\circ$ (Fig. 6(b) and (c)). Though the surfaces for the 5-qp configuration (Fig. 6(c)) shows a stable triaxial minimum with $\gamma = 31^\circ$, the surfaces for the 3-qp configuration shows some degree of γ-softness with two close-by minima; the first minimum is at $\gamma = 39^\circ$ and the second minimum, lying at about 1 MeV above the first one, is at the oblate deformation with $\gamma = -64^\circ$. It may be noted that although the tilted axis cranking (TAC) calculations give a better estimate for the realization of the chiral geometry in a nucleus [2] with rotation around a tilted axis, but the present TRS calculations using principal axis cranking (PAC) are good to predict the triaxial shapes, a requirement for the realization of the chiral geometry. The stable triaxial minimum for the 5-qp configuration gives the possibility of the nucleus to rotate around its intermediate axis and results in degenerate doublet bands as observed for B4-B4a pair of bands in ^{195}Tl. In case of 3-qp configuration, the triaxial minimum which lies lower in energy can provide the required chiral condition for the occurrence of doubly degenerate bands in B2 and B2a, however, because of the second co-existing minimum and a small degree of γ-softness, the chiral conditions quickly gets destroyed and hence, the degenerate bands are expected in a limited region as is the case for the B2-B2a pair of bands.

The well defined stable triaxial minimum for the 5-qp band in ^{195}Tl is comparable to some of the best known chiral doublet bands in $A = 130$ region in which the proton particle and neutron hole lie in the high-j $h_{11/2}$ orbitals [3]. Therefore, from the TRS calculations it turns out that likewise for the nuclei in $A = 130$ region, doubly degenerate band, originated due to the chiral symmetry breaking, is expected for the 5-qp band in ^{195}Tl. Once the nucleus is triaxial in this $A = 190$ region, the chiral geometry will be better realized because of the involvement of the higher-j $i_{13/2}$ orbital. This is in excellent agreement with the experimental observation in case of bands B4 and B4a in ^{195}Tl and represents one of the best cases of doubly degenerate band structures. It may however, be noticed that a stable triaxial shape is realized in this case only when several neutron holes are available in the $i_{13/2}$ orbital.

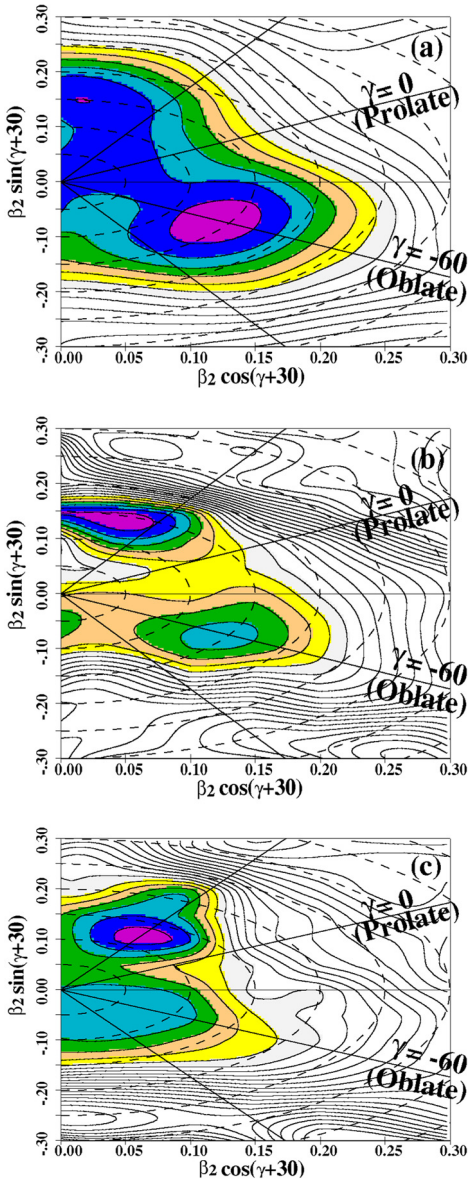

Fig. 6. Calculated total Routhian surfaces (TRS) for ^{195}Tl in the β_2–γ deformation mesh for the configurations of bands B1 (a), B2 (b) and B4 (c). The contours are 500 keV apart.

In summary, the study of the higher spin states in the nucleus ^{195}Tl by the heavy-ion induced reaction reveals the evidence for the presence of multiple chiral doublet bands in this nucleus based on 3-qp and 5-qp configurations. This is the first time that MχD bands are observed in a nucleus in heavy mass region with $A > 150$ and only the fourth such evidence in the chart of nuclide. It indicates the presence of triaxial shape coexistence in ^{195}Tl, which was reproduced well in the microscopic-macroscopic calculations of the TRS. The calculations also give an important conclusion that a stable triaxial shape of ^{195}Tl is realized only for a configuration with large number of neutron holes (four in case of ^{195}Tl) in the $i_{13/2}$ orbital. Therefore, the predicted chiral geometry in $A = 190$ region can be realized only for the large quasi-neutron configurations involving the $i_{13/2}$ orbital. That may be the reason

the experimental observation of chiral geometry was so far almost illusive in this region as it is experimentally difficult to produce and observe the multi-quasiparticle high spin states in this region. The experimental observation of the excellent degeneracy, possibly the best observed so far, between the doubly degenerate chiral partner bands for the 5-qp configuration in ^{195}Tl in this work, supports the conclusion of the original prediction of Ref. [1] that $A = 190$ region is one of the best regions to realize chiral geometry in nuclei. Further investigation needs to be carried out in other nuclei in this mass region to establish this fact. Although the PAC calculations give a good account of the triaxial shapes for the two configurations in ^{195}Tl, but it will be interesting to perform the TAC calculations, particularly for the 3-qp band in order to estimate the shape for tilted axis rotation.

Acknowledgements

The authors gratefully acknowledge the effort of the pelletron operators at BARC-TIFR (PLF), Mumbai for providing a good quality of ^{13}C beam. We thank all the members of INGA collaboration for setting up the array. Financial support of Department of Science & Technology, Govt. of India for clover detectors of INGA (Grant No. IR/S2/PF-03/2003-II) is greatfully acknowledged. One of the authors (S. Bhattacharya) acknowledges with thanks the financial support received as Raja Ramanna Fellowship from the Department of Atomic Energy, Govt. of India. T.R and Md. A.A acknowledge with thanks the financial support received as research fellows from the Department of Atomic Energy (DAE), Govt. of India.

References

[1] S. Frauendorf, J. Meng, Nucl. Phys. A 617 (1997) 131.
[2] S. Frauendorf, Rev. Mod. Phys. 73 (2001) 463.
[3] K. Starosta, et al., Phys. Rev. Lett. 86 (2001) 971.
[4] C. Vaman, et al., Phys. Rev. Lett. 92 (2004) 032501.
[5] J. Sethi, et al., Phys. Lett. B 725 (2013) 85.
[6] J. Timar, et al., Phys. Rev. C 73 (2006) 011301(R).
[7] S. Zhu, et al., Phys. Rev. Lett. 91 (2003) 132501.
[8] C.M. Petrache, et al., Phys. Rev. C 97 (2018) 041304(R).
[9] J.A. Alcántara-Núñez, et al., Phys. Rev. C 69 (2004) 024317.
[10] J. Timar, et al., Phys. Lett. B 598 (2004) 178.
[11] J. Meng, J. Peng, S.Q. Zhang, S-G. Zhou, Phys. Rev. C 73 (2006) 037303.
[12] A.D. Ayangeakaa, et al., Phys. Rev. Lett. 110 (2013) 172504.
[13] C. Liu, et al., Phys. Rev. Lett. 116 (2016) 112501.
[14] I. Kuti, et al., Phys. Rev. Lett. 113 (2014) 032501.
[15] L. Esser, U. Neuneyer, R.F. Casten, P. von Brentano, Phys. Rev. C 55 (1997) 206.
[16] P.L. Masiteng, et al., Phys. Lett. B 719 (2013) 83.
[17] P.L. Masiteng, et al., Eur. Phys. J. A 52 (2016) 28.
[18] E.A. Lawrie, et al., Phys. Rev. C 78 (2008) 021305(R).
[19] R.M. Lieder, et al., Nucl. Phys. A 299 (1978) 255.
[20] R. Palit, et al., Nucl. Instrum. Methods Phys. Res. A 680 (2012) 90.
[21] H. Tan, et al., in: Nuclear Science Symposium Conference Record 2008, IEEE, Washington, DC, 2008, p. 3196.
[22] H. Pai, et al., Phys. Rev. C 85 (2012) 064313.
[23] K. Starosta, et al., Nucl. Instrum. Methods Phys. Res. A 423 (1999) 16.
[24] Ch. Droste, et al., Nucl. Instrum. Methods Phys. Res. A 378 (1996) 518.
[25] A. Krämer-Flecken, et al., Nucl. Instrum. Methods Phys. Res. A 275 (1989) 333.
[26] G.J. Lane, et al., Nucl. Phys. A 586 (1995) 316.
[27] M.G. Porquet, et al., Phys. Rev. C 44 (1991) 2445.
[28] W. Reviol, et al., Phys. Scr. T 56 (1995) 167.
[29] W. Reviol, et al., Nucl. Phys. A 548 (1992) 331.
[30] H. Hübel, et al., Nucl. Phys. A 453 (1986) 316.
[31] H. Pai, et al., Phys. Rev. C 84 (2011) 041301(R).
[32] W. Nazarewicz, et al., Nucl. Phys. A 435 (1985) 397.
[33] W. Nazarewicz, et al., Nucl. Phys. A 512 (1990) 61.
[34] T. Roy, et al., Eur. Phys. J. A 51 (2015) 153.
[35] G. Mukherjee, et al., Nucl. Phys. A 829 (2009) 137.